Chemical Modification of the Urokinase-Type Plasminogen Activator and Its Receptor Using Tetranitromethane. Evidence for the Involvement of Specific Tyrosine Residues in Both Molecules during Receptor−Ligand Interaction†

Michael Ploug,*,‡ Henrik Rahbek-Nielsen,§ Vincent Ellis,|| Peter Roepstorff,§ and Keld Danø‡

Finsen Laboratory, Rigshospitalet, Strandboulevarden 49, DK-2100 Copenhagen Ø, Denmark, Department of Molecular Biology, Odense University, Campusvej 55, DK-5230 Odense M, Denmark, and Thrombosis Research Institute, Emmanuel Kaye Building, Manresa Road, London SW3 6LR, U.K.

Received April 17, 1995; Revised Manuscript Received June 26, 1995⊗

ABSTRACT: The high-affinity interaction between urokinase-type plasminogen activator (uPA) and its glycolipid anchored receptor (uPAR) is essential for the confinement of plasminogen activation to cell surfaces where it is thought to play an important role in cancer cell invasion and metastasis. The receptor binding site of uPA is retained within its isolated growth factor-like module (GFD; residues 4−43). The NH_2-terminal domain of uPAR has a primary role in uPA binding, although maintenance of its multidomain structure has been shown to be necessary for the high affinity of this interaction [Ploug, M., Ellis, V., & Danø, K. (1994) *Biochemistry 33*, 8991−8997]. To identify residues engaged in the uPAR−uPA interaction, we have performed a "protein−protein footprinting" study on preformed uPAR−GFD complexes by chemical modification with tetranitromethane. All six tyrosine residues in uPAR and the single tyrosine residue in GFD (Tyr^{24}) were susceptible to nitration in the native uncomplexed proteins, whereas in the receptor−ligand complexes both Tyr^{57} of uPAR and Tyr^{24} of GFD were protected from modification. Modification of uPAR alone led to a parallel reduction in the potential to bind pro-uPA and 8-anilino-1-naphthalenesulfonate, an extrinsic fluorophore reporting on the accessibility of a hydrophobic site involved in uPA binding. These data clearly demonstrate that Tyr^{57} in the NH_2-terminal domain of uPAR and Tyr^{24} in uPA are intimately engaged in the receptor−ligand interaction, whereas Tyr^{87} positioned in the linker region between the first two domains of uPAR does not appear to be shielded by the resulting intermolecular interface.

The ability to degrade extracellular matrix proteins is one of the important hallmarks of the malignant phenotype of tumor cells being used during invasive and metastatic spread. Several studies imply that plasminogen activation catalyzed by the urokinase-type plasminogen activator (uPA)[1] contributes significantly to this phenotype either directly or indirectly by activation of matrix metalloproteinases such as stromelysin (Murphy et al., 1992, Danø et al., 1994). Due to the high-affinity association of uPA to cells ($K_d \approx 0.1-1$ nM) via specific binding to its cellular receptor (uPAR), activation of this system is confined to the microenvironment of the surface of uPAR expressing cells (Ellis et al., 1992).

Human uPAR is a glycolipid-anchored membrane glycoprotein (Ploug et al., 1991a) encoded as a 335-residue polypeptide (Roldan et al., 1990), but during posttranslational processing it is truncated due to the removal of the NH_2-terminal signal sequence (22 residues) and a COOH-terminal sequence responsible for the addition of the glycosylphosphatidylinositol moiety (presumably 26 residues). The entire sequence of this fully processed and completely extracellular uPAR (residues 1−283) is divided into three homologous domains primarily defined by a conserved pattern of cysteine residues (Behrendt et al., 1991; Ploug et al., 1991b). Murine, bovine, and rat cDNA's encoding proteins with similar properties have also been reported (Kristensen et al., 1991; Krätzschmar et al., 1993; Rabbani et al., 1994). A structural relationship of the individual uPAR domains to a functionally diverse group of glycolipid anchored, single-domain proteins (CD59, Ly-6, HSV-15, and ThB) conforming to the consensus sequence derived from the three repeats of uPAR has been identified (Behrendt et al., 1991; Palfree 1991; Ploug et al., 1991b). Determination of the disulfide bond pattern of the NH_2-terminal domain of uPAR (Ploug et al., 1993) further validated this relationship and also revealed a potential structural similarity to the secreted single-domain snake venom α-neurotoxins and their homologs (Ploug & Ellis, 1994). Several three-dimensional structures of α-neurotoxins have been solved showing considerable similarity to the solution structure of CD59, the only member of the Ly-6/uPAR family analyzed at this level (Fletcher et al., 1994; Kieffer et al., 1994).

The specific, high-affinity interaction between uPAR and uPA is governed entirely by the growth factor-like module (GFD) of uPA, a mosaic protein which also contains a kringle

† This work was supported financially by the Danish Cancer Society and the Danish Biotechnology Program.

* Address correspondence to this author at Finsen Laboratory, Rigshospitalet Opg. 86.21, Strandboulevarden 49, DK-2100 Copenhagen Ø, Denmark (telephone, +45-35455708; FAX, +45-31385450).
‡ Finsen Laboratory.
§ Odense University.
|| Thrombosis Research Institute.

⊗ Abstract published in *Advance ACS Abstracts,* September 1, 1995.

[1] Abbreviations: ANS, 8-anilino-1-naphthalenesulfonic acid; ATF, amino-terminal fragment of uPA; GFD, growth factor-like domain of uPA; MALDI-MS, matrix-assisted laser desorption ionization mass spectrometry; PD-MS, plasma desorption mass spectrometry; PVDF, poly(vinylidene difluoride); TNM, tetranitromethane; uPA, urokinase-type plasminogen activator; uPAR, uPA receptor.

0006-2960/95/0434-12524$09.00/0

module and a serine protease domain. The recently solved solution structure of the amino-terminal fragment of uPA (containing the GFD and kringle modules) provides an explanation for this discrete localization of the major binding determinants, as the kringle and GFD modules exhibit a complete structural independence with no interdomain interactions (Hansen et al., 1994a). In contrast to this, the multidomain structure of uPAR is essential for high-affinity binding to uPA (Ploug et al., 1994). Although little is known about the structural properties of the ligand binding site on uPAR, several experiments indicate that the NH_2-terminal domain I of uPAR has the primary role in uPA binding (Behrendt et al., 1991; Rønne et al., 1991). This domain does, however, not contain all determinants necessary for high-affinity binding as there appears to be a critical requirement for interdomain interactions, which may be either directly or indirectly involved in ligand binding (Ploug et al., 1994).

The study of the three-dimensional structure of uPAR is likely to prove difficult for a variety of reasons. X-ray crystallographic studies will probably be hampered by the reluctance of uPAR to form crystals due to the presence of a large amount of heterogeneous carbohydrate with an average mass of 9700 Da as measured by MALDI-MS (Ploug and Rahbek-Nielsen, unpublished data). As with CD59 (Fletcher et al., 1994), the solution structure of the isolated NH_2-terminal domain I of uPAR is presumably amenable to determination by NMR, but such data may be of limited value since this domain exhibits negligible ligand-binding affinity when removed from domains II and III (Ploug et al., 1994). In the present study we have therefore adopted the approach of "protein−protein footprinting" by specific chemical modification using tetranitromethane to determine putative tyrosine residues in either intact uPAR or GFD found at the intermolecular interface of the receptor−ligand complex.

MATERIALS AND METHODS

Chemicals and Reagents. Tetranitromethane (TNM) was from Aldrich Chemical Co. (Steinheim, Germany). 3-Nitro-L-tyrosine and 8-anilino-1-naphthalenesulfonic acid (ANS) were from Sigma (St. Louis, MO). ANS was stored as a stock solution of 100 mg/mL in water and its molar concentration determined spectrophotometrically using $\epsilon_{386nm} = 3985\ M^{-1}\ cm^{-1}$.

Purified Proteins. Recombinant pro-uPA (EC 3.4.21.31) expressed in *Escherichia coli* was a kind gift from Dr. D. Saunders (Grünenthal, Germany). The growth factor-like module (residues 4−43) was generated from pro-uPA by Glu-C digestion in 0.2 M NH_4HCO_3 (pH 8.0) for 6 h at 37 °C using an enzyme to substrate ratio of 1:20 (w/w) according to the procedure of Mazar et al. (1992). The released GFD was subsequently purified by gel filtration chromatography using a Superdex 30 HiLoad column followed by reversed-phase chromatography on a ProRPC HR5/10 column (both from Pharmacia LKB Biotechnology Inc., Uppsala, Sweden). The GFD preparation obtained by this procedure was intact and of high purity as measured by MALDI-MS (one dominant peak with a mass assignment of 4462.5 Da; see Figure 3A) and was functionally active as assessed by its ability to stoichiometrically titrate the specific uPAR enhancement of ANS fluorescence (Ploug et al., 1994). A soluble, truncated uPAR derivative (residues 1−277) was purified by immunoaffinity chromatography from the conditioned media of transfected Chinese hamster ovary cells (Ploug et al., 1993) and quantified spectrophotometrically using $E^{1\%}_{280nm} = 9.2$ (Rønne et al., 1994). Monoclonal antibodies to human uPAR (R2, R3, and R8) were produced and characterized as described previously (Rønne et al., 1991).

Modified porcine trypsin (EC 3.4.21.4) of sequencing grade was purchased from Promega (Madison, WI), and the endoproteinase Glu-C (EC 3.4.21.19) from *Staphylococcus aureus* V8 was from ICN ImmunoBiologicals (Costa Mesa, CA). Pro-uPA was labeled with biotin using a molar ratio of 1:1; the resultant modification did not influence its receptor binding properties significantly.

Nitration of uPAR and uPAR−GFD Complexes. Specific nitration of tyrosine residues was performed essentially as described by Sokolovsky et al. (1966). Aliquots from a freshly prepared stock solution of 25 mM TNM in 96% ethanol were mixed thoroughly with 200 μL of 0.1 M NH_4HCO_3 (pH 8.0) containing 20−30 μM uPAR (free or in complex with GFD). Nitration proceeded for 60 min at 25 °C and was subsequently terminated by gel filtration chromatography. This procedure separated modified, monomeric uPAR from varying amounts of dimeric, cross-linked protein, as well as excess reagent and nitroformate. The extent of nitration achieved was measured both spectrophotometrically using $\epsilon_{428nm} = 4100\ M^{-1}\ cm^{-1}$ for 3-nitrotyrosine at alkaline pH (Sokolovsky et al., 1966) and by amino acid composition analysis.

Enzymatic Cleavage of uPAR. To liberate uPAR domain I from domains II + III, the chemically modified uPAR preparations were incubated with trypsin in 0.2 M NH_4HCO_3 (pH 8.0) using an enzyme to substrate ratio of 1:2000 (w/w) for 1 h at 37 °C. This treatment quantitatively excised the peptide Ala^{84}-Val-Thr-Tyr-Ser-Arg^{89} from the linker region separating domains I and II, thus liberating domain I from domains II + III. Further cleavage of isolated domain I (residues 1−83) was obtained by increasing the trypsin concentration to a ratio of 1:25 (w/w).

Chromatographic Conditions. Gel filtration analyses were performed in 0.1 M NH_4HCO_3 (pH 8.0) using a Superdex 75 HR10/30 column (Pharmacia LKB Biotechnology Inc.) at a flow rate of 500 μL/min. The effluent was monitored at both 214 and 436 nm to obtain specific signals for peptides containing 3-nitrotyrosine.

Two different reversed-phase HPLC columns (pore sizes 300 Å) were employed. In order to dissociate and separate GFD in complex with uPAR, samples were initially acidified by addition of TFA, then loaded onto a dual bonded C1/C8 + C2/C8 ProRPC HR5/2 column (Pharmcia LKB Biotechnology Inc.), and finally eluted with a linear gradient of 0.1% (v/v) TFA in water to 70% (v/v) 2-propanol containing 0.085% (v/v) TFA at a flow rate of 300 μL/min. The smaller peptides originating from the trypsin degradation were separated on a Brownlee Aquapore OD-300 C18 column (2.1 × 100 mm) using a 50-min linear gradient from 0 to 70% (v/v) acetonitrile in 0.1% and 0.085% (v/v) TFA, respectively, at a flow rate of 250 μL/min. During reversed-phase chromatography detection was at 214 and 365 nm as the absorption maximum of 3-nitrotyrosine is blue shifted upon acidification (Sokolovsky et al., 1966).

Functional Integrity of uPAR Measured by ELISA. Interaction of uPAR with pro-uPA and various monoclonal antibodies was measured using a modified version of a previously published ELISA method for quantitation of uPAR in biological fluids (Rønne et al., 1994). In brief, a monoclonal anti-uPAR antibody (R8) recognizing domain II + III of uPAR was used as catching antibody for a 2-fold dilution series of either purified TNM-treated uPAR or mock-treated uPAR as control. Biotinylated R2 (recognizing domain II + III of uPAR), R3 (recognizing the NH_2-terminal domain I of uPAR), and pro-uPA (1 nM) were used as detecting ligands. The interactions were subsequently visualized using peroxidase-labeled streptavidin. To ensure that nitration did not affect binding of uPAR to the catching antibody, at least one of the ligands should react independently of the chemical modification.

ANS Fluorescence Measurements. Fluorescence emission spectra of ANS were obtained on a Perkin-Elmer LS-5 spectrofluorometer using an excitation wavelength of 386 nm and recording emission at 470 nm, using 5-nm band-pass excitation and emission slits and 5 mm path-length quartz cuvettes. All fluorescence measurements were made using 1 μM uPAR and 10 μM ANS in 0.1 M NH_4HCO_3 (pH 8.0) at 25 °C (Ploug et al., 1994).

Amino Acid Analysis. Amino acid analysis was performed on a Waters amino acid analyzer, equipped with *o*-phthaldialdehyde derivatization essentially as described (Barkholt & Jensen, 1989). Quantitation of 3-nitrotyrosine was obtained indirectly by subtracting the measured tyrosine content from the theoretical value as 3-nitrotyrosine does not yield any fluorescent derivative detectable in the *o*-phthaldialdehyde system. In certain cases amino acid analyses were performed on samples hydrolyzed *in situ* on PVDF membranes, onto which they were transferred by electroblotting after SDS–PAGE (Ploug et al., 1992).

Mass Spectrometry. Plasma desorption mass spectrometry (PD-MS) was performed on a BioIon 20K instrument (Applied Biosystems AB, Uppsala, Sweden) according to the procedure of Sundqvist et al. (1984). Samples were applied onto nitrocellulose-coated targets and dried by the spin drying procedure (Roepstorff, 1994). Data were accumulated for 10^6 desorption events and internally calibrated on peaks of H^+ and NO^+. *Matrix-assisted laser desorption ionization mass spectrometry* (MALDI-MS) was performed on a linear time-of-flight mass spectrometer (Applied Biosystems AB, Uppsala, Sweden) equipped with a 0.7 m flight tube and a 337 nm nitrogen laser using 1.5% (w/v) α-cyano-4-hydroxycinnamic acid in 70% acetonitrile as matrix (Beavis et al., 1992). The probe tip was precoated with 0.5 μL of matrix solution and dried before equal volumes of the sample and matrix were mixed on the probe tip and dried at ambient temperature. Each MALDI spectrum represents data accumulated from 50 laser shots. The instrument was externally calibrated using human insulin just prior to recording the spectra of GFD.

RESULTS

Nitration of uPAR by TNM. In the present study we used tetranitromethane as a modifying reagent in a receptor–ligand protection assay to delineate specific tyrosine residues involved in the high-affinity interaction between uPAR and uPA. The reason for choosing this reagent is twofold. Under mild conditions TNM is an efficient and specific reagent for the nitration of solvent-accessible tyrosine residues (Sokolovsky et al., 1966; Cuatrecasas et al., 1968), and previous spectroscopic studies have indicated the possible involvement of aromatic residues in the uPAR–uPA interaction (Ploug et al., 1994). In the following nitration experiments we used a purified soluble uPAR lacking the glycolipid anchor (residues 1–277) and secreted from Chinese hamster ovary cells as a convenient source of receptor–protein, which will subsequently be referred to simply as uPAR. We have previously demonstrated that this recombinant uPAR variant binds uPA with an affinity similar to that of the cell surface glycolipid anchored uPAR (Ploug et al., 1994). The extent of 3-nitrotyrosine formation in uPAR as a function of the molar excess of TNM at pH 8.0 is shown in Figure 1A. In contrast to certain other proteins (Lundblad & Noyes, 1984),

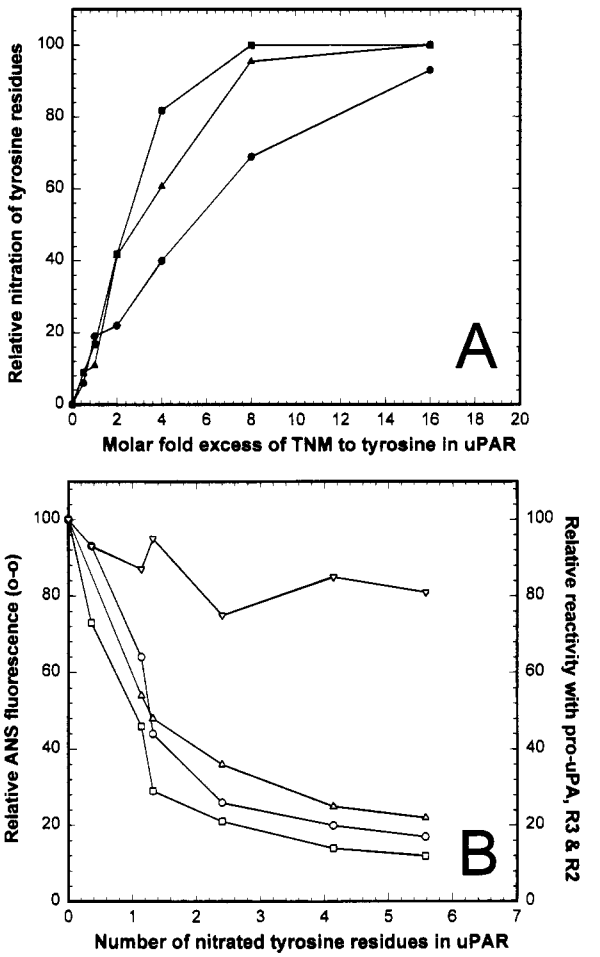

FIGURE 1: Titration of uPAR with TNM: tyrosine nitration and its consequence for the functional properties of uPAR. (A) After nitration of intact uPAR (30 μM) with varying concentrations of TNM (0–2.8 mM) monomeric uPAR was purified by gel filtration chromatography. Shown is the estimated degree of nitration achieved as measured spectrophotometrically using absorbance at both 280 and 428 nm (●). The specific nitration of Tyr^{57} (▲) and Tyr^{87} (■) was calculated from experiments similar to those outlined in Figures 2 and 4. (B) Various functional properties of modified uPAR are shown as a function of the average number of tyrosine residues nitrated (uPAR contains a total of six tyrosine residues). The residual activities are expressed relative to a mock-treated control preparation. The following properties of uPAR were tested: enhancement of ANS fluorescence (○), reactivity with 1 nM pro-uPA in a ligand ELISA (□), and immunoreactivity against two monoclonal anti-uPAR antibodies, R3 (△) and R2 (▽), also by ELISA.

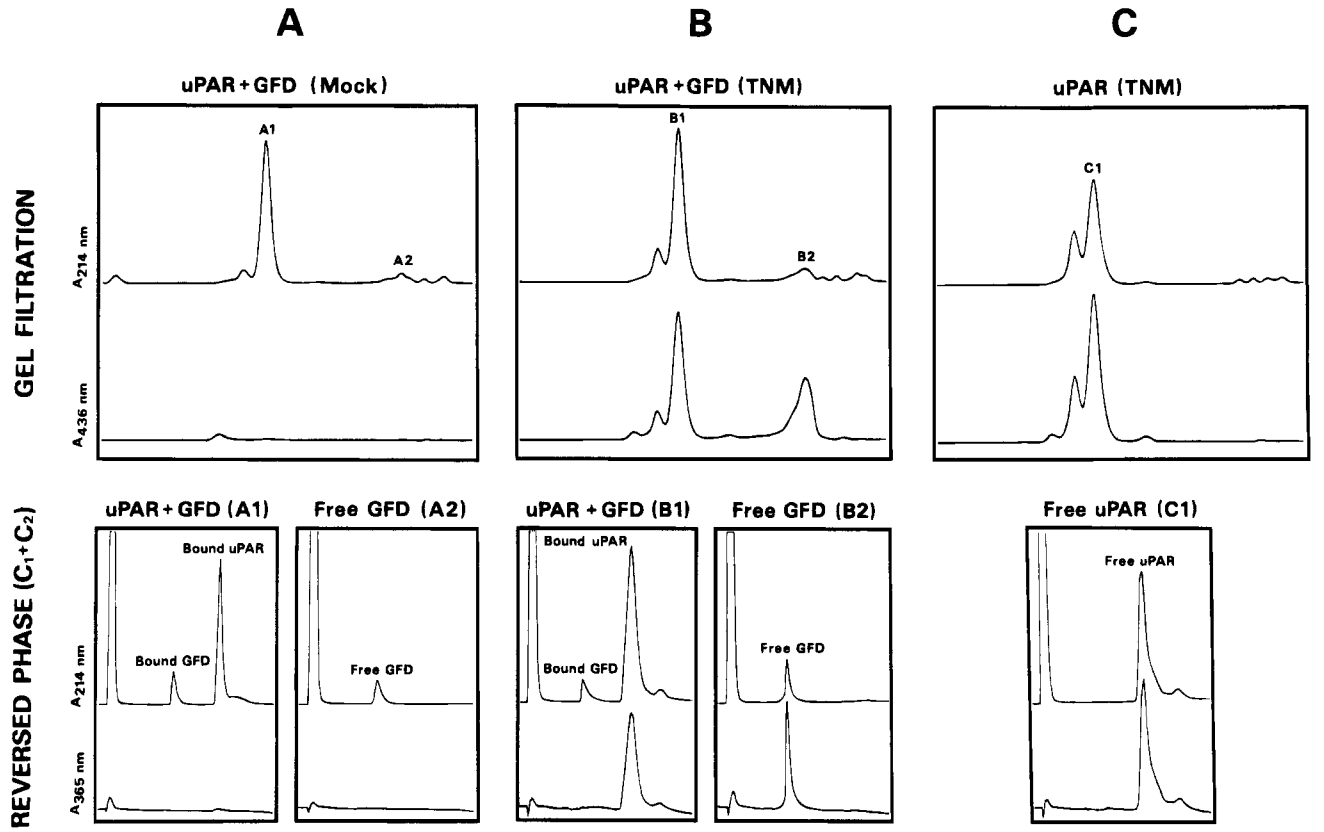

FIGURE 2: Nitration of uPAR−GFD complexes followed by dissociation and purification of the individual components. After a 15 min preincubation of uPAR (20 μM) with an excess of GFD (40 μM) nitration was performed using a 4-fold molar excess of TNM compared to the total content of tyrosine. Shown in the upper panel are gel filtration analyses of uPAR−GFD complexes (columns A and B) and uncomplexed uPAR (column C) treated with TNM (columns B and C). Shown in the lower panel are the reversed-phase chromatograms of fractions corresponding to uPAR−GFD complexes (A1 and B1), free uPAR (C1), and free GFD (A2 and B2) obtained from the gel filtration experiments described in the upper panel. Elution profiles were monitored at 214 nm for the detection of peptides and at 436 nm (gel filtration, pH 8) or 365 nm (reversed phase, pH <2) for the specific detection of nitrotyrosine.

Table 1: Amino Acid Composition and MALDI-MS Analyses of Free and Receptor-Bound GFD with and without Previous Nitration Using TNM[a]

sample	bound GFD mock (A1)	free GFD mock (A2)	bound GFD 4 × TNM (B1)	free GFD 4 × TNM (B2)
Asx	6.29 (6)	6.23 (6)	6.22 (6)	6.36 (6)
Thr	1.01 (1)	1.01 (1)	1.00 (1)	1.06 (1)
Ser	3.03 (3)	2.97 (3)	2.97 (3)	3.11 (3)
Glx	3.06 (3)	3.10 (3)	3.11 (3)	3.19 (3)
Pro	2.07 (2)	2.12 (2)	2.15 (2)	2.19 (2)
Gly	4.27 (4)	4.26 (4)	4.31 (4)	4.39 (4)
Ala	0.05 (0)	0.06 (0)	0.06 (0)	0.04 (0)
Cys[b]	5.22 (6)	5.12 (6)	5.29 (6)	5.42 (6)
Val	2.07 (2)	2.11 (2)	2.07 (2)	2.11 (2)
Met	0.01 (0)	0.03 (0)	0.00 (0)	0.02 (0)
Ile	0.69 (1)	0.77 (1)	0.71 (1)	0.67 (1)
Leu	2.13 (2)	2.17 (2)	2.12 (2)	2.19 (2)
Tyr[c]	**1.03 (1)**	**1.02 (1)**	**1.00 (1)**	**0.12 (1)**
Phe	2.09 (2)	2.08 (2)	2.09 (2)	2.11 (2)
His	2.81 (3)	2.84 (3)	2.80 (3)	2.79 (3)
Lys	3.16 (3)	3.12 (3)	3.13 (3)	3.22 (3)
Arg	0.02 (0)	0.05 (0)	0.04 (0)	0.01 (0)
Trp	nd (1)	nd (1)	nd (1)	nd (1)
MALDI-MS[d] (4464.0 Da)	4464.4 (Δm = 0.4)	4461.5 (Δm = −2.5)	4464.0 (Δm = 0.0)	4492.9 (Δm = 28.9) 4508.7 (Δm = 44.7)

[a] Values in parentheses correspond to the theoretical number of residues in GFD (residues 4−43) calculated from the amino acid sequence of human uPA (Günzler et al., 1982). [b] Cysteine was determined as the mixed disulfide formed between cystine and 3,3′-dithiodipropionic acid during hydrolysis (Barkholt & Jensen, 1989). [c] When a nitrated hexapeptide (AVTY[NO_2]SR) was hydrolyzed and analyzed by amino acid analysis, no fluorescent compound originating from 3-nitrotyrosine was detected. Likewise authentic 3-nitro-L-tyrosine analyzed directly without hydrolysis did not yield any fluorescent signal either. [d] One atomic mass unit has been subtracted from the recorded masses of each molecular ion (MH^+) due to the association of one proton during ionization. Deviations from the theoretical mass of GFD (4464.0 Da) are shown in parentheses.

polymerization of uPAR induced by the TNM treatment did not pose serious problems since the higher TNM concentrations only caused an approximately 30% dimerization of uPAR as evaluated by gel filtration chromatography (data

not shown). At a 16-fold molar excess of TNM an average of five to six tyrosine residues in uPAR (out of six in total) were derivatized to 3-nitrotyrosine; it cannot be excluded, however, that a single tyrosine residue was partially resistant to nitration.

As the involvement of uPAR domain I in ligand binding has been demonstrated unambiguously (Behrendt et al., 1991; Rønne et al., 1991), we particularly wanted to characterize the reactivities of Tyr^{57} and Tyr^{87} to nitration. The various monomeric uPAR preparations from the titration experiment described in Figure 1A were therefore cleaved with trypsin under mild conditions, liberating domain I (residues 1−83) and a tyrosine-containing hexapeptide derived from the interdomain linker region (residues 84−89). The isolated domain I was further degraded using a higher trypsin concentration, and the liberated peptides were subsequently analyzed by reversed-phase chromatography in an experiment similar to that outlined in Figure 4. The extent of nitration of Tyr^{57} and Tyr^{87} was measured by amino acid analysis and is shown in Figure 1A. Both tyrosine residues were readily derivatized by TNM and completely converted to 3-nitrotyrosine at an 8-fold molar excess of TNM, although Tyr^{57} appears to react slightly less efficiently than Tyr^{87}.

The impact of tyrosine nitration on the ligand binding properties of uPAR was analyzed in a ligand binding ELISA in which biotinylated pro-uPA (1 nM) was used to probe the binding properties of the preparations of monomeric but heterogeneously nitrated uPAR (samples from the experiment in Figure 1A). Under these conditions, as shown in Figure 1B, an average nitration of two to three tyrosine residues (obtained at a 4−5-fold molar excess of TNM) inhibited pro-uPA binding to the modified uPAR by approximately 80%. The ability of uPAR to bind an anti-uPAR monoclonal antibody (R3), which recognizes domain I of uPAR and interferes with pro-uPA binding, was similarly affected. Also shown in Figure 1B is the observation that the specific enhancement of ANS fluorescence on binding to uPAR (Ploug et al., 1994) was also reduced by the TNM modification in proportion to the loss of uPA binding.

Nitration of uPAR−GFD Complexes by TNM. To probe the intermolecular interface between uPAR and uPA for the presence of tyrosine residues, uPAR was preincubated with a 2-fold molar excess of GFD (the receptor binding module of uPA) for 15 min before the addition of TNM. We chose to use a 4-fold molar excess of TNM relative to the total content of tyrosine as this ratio was predicted to cause an average nitration of two to three tyrosines in uPAR to which both Tyr^{57} and Tyr^{87} contribute significantly, having estimated nitration efficiencies of 60% and 80%, respectively (Figure 1A). In addition, the major impairment of the functional properties of uPAR has already occurred at this ratio of TNM with little or no effect on further nitration (Figure 1B).

uPAR−GFD complexes were separated from excess GFD by gel filtration (Figure 2, upper panel), which also resolved the TNM-induced uPAR dimers. It was consistently observed that this dimer formation was less pronounced with the uPAR−GFD complexes than with uPAR alone. Nitration detected by absorbance was observed in uPAR (C1), the uPAR−GFD complex (B1), and uncomplexed GFD (B2). These peaks were collected and subjected to further analysis on reversed-phase HPLC after acidification to dissociate uPAR−GFD complexes.

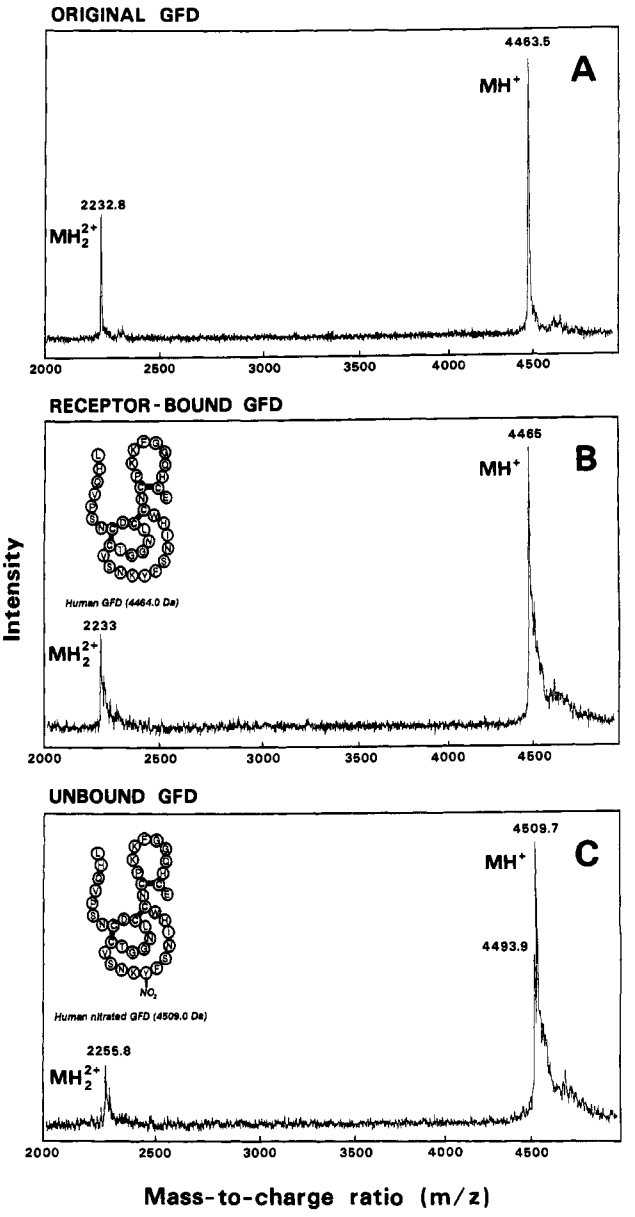

FIGURE 3: MALDI-MS analysis of the GFD modules recovered from the chemical protection analysis using TNM. Panel A shows the MALDI-MS spectrum of the original preparation of the GFD module (residues 4−43) derived by Glu-C cleavage from recombinant pro-uPA expressed in *E. coli*. Panels B and C show the MALDI-MS spectra of this GFD preparation subjected to a chemical protection assay using TNM as modifying reagent; panel B is receptor-bound GFD (derived from B1 in Figure 2), and panel C is the corresponding unbound fraction of GFD derived from the same modification experiment (B2 in Figure 2).

Receptor Protection of GFD during Chemical Modification. The chromatograms in Figure 2B (lower panel) show that the GFD dissociated from the complex with uPAR had no detectable nitration determined by absorbancy in contrast to the nitration of uncomplexed GFD noted above. When this uncomplexed GFD was similarly subjected to acidification and reversed-phase HPLC, it retained its nitration, demonstrating that the lack of GFD nitration in the complex was not caused by chemical lability of the 3-nitrotyrosine but was due to a true protection of the single tyrosine residue in GFD on interaction with uPAR. The validity of this conclusion is dependent on the homogeneity and integrity of the GFD preparation, ruling out the possible presence of

Table 2: Amino Acid Composition Analyses of Free and Ligand-Bound uPAR with and without Previous Nitration Using TNM[a]

	intact uPAR (samples from Figure 2)[b]			uPAR domains II-III (samples from Figure 4)[c]		
sample	mock (A1)	4 × TNM (B1)	4 × TNM (C1)	mock (A3)	4 × TNM (B3)	4 × TNM (C3)
Asx	30.0 (29)	30.2 (29)	30.4 (29)	22.9 (22)	23.3 (22)	22.7 (22)
Thr	19.9 (20)	19.4 (20)	19.8 (20)	9.9 (10)	10.1 (10)	10.0 (10)
Ser	23.1 (23)	23.6 (23)	23.7 (23)	16.6 (17)	17.5 (17)	17.0 (17)
Glx	35.0 (35)	34.3 (35)	35.1 (35)	21.7 (22)	22.8 (22)	22.4 (22)
Pro	9.6 (9)	9.8 (9)	10.3 (9)	9.6 (9)	10.0 (9)	9.8 (9)
Gly	26.6 (25)	27.8 (25)	28.0 (25)	19.0 (18)	20.2 (18)	19.9 (18)
Ala	7.6 (7)	7.8 (7)	8.0 (7)	5.3 (5)	5.6 (5)	5.6 (5)
Cys	26.6 (28)	25.6 (28)	24.1 (28)	21.4 (20)	19.8 (20)	19.3 (20)
Val	8.7 (11)	9.1 (11)	8.6 (11)	4.1 (5)	4.2 (5)	4.4 (5)
Met	6.3 (6)	5.9 (6)	6.0 (6)	3.9 (5)	4.0 (5)	3.5 (5)
Ile	6.1 (7)	6.2 (7)	6.4 (7)	4.4 (5)	4.5 (5)	4.5 (5)
Leu	25.3 (24)	24.6 (24)	24.7 (24)	13.2 (13)	13.6 (13)	13.4 (13)
Tyr	**6.2 (6)**	**4.3 (6)**	**3.6 (6)**	**4.0 (4)**	**3.3 (4)**	**3.0 (4)**
Phe	5.1 (5)	5.3 (5)	5.2 (5)	5.0 (5)	5.2 (5)	5.1 (5)
His	12.2 (12)	12.1 (12)	12.1 (12)	11.2 (11)	11.2 (11)	11.0 (11)
Lys	10.4 (10)	10.9 (10)	10.5 (10)	6.3 (6)	6.5 (6)	6.4 (6)
Arg	18.3 (18)	17.8 (18)	17.8 (18)	10.1 (10)	10.3 (10)	10.2 (10)
Trp	nd (2)	nd (2)	nd (2)	nd (1)	nd (1)	nd (1)

[a] Values in parentheses correspond to the number of amino acids in either intact $uPAR_{I-III}$ (residues 1−277) or trypsin derived $uPAR_{II-III}$ (residues 90−277) according to the cDNA-derived amino acid sequence (Roldan et al., 1990). [b] Aliquots from the ProRPC reversed-phase chromatographies (Figure 2, lower panel) were dried, hydrolyzed, and analyzed directly using 3,3′-dithiodipropionic acid for cysteine determination (Barkholt & Jensen, 1989). [c] Aliquots from the Superdex 75 gel filtration chromatographies (Figure 4, upper panel) were dried, analyzed by SDS−PAGE, electroblotted onto PVDF membranes, Coomassie stained, and hydrolyzed *in situ* on the membrane (Ploug et al., 1992). Cysteine was determined after alkylation with iodoacetamide.

a discrete subpopulation of GFD which is unable to bind uPAR but highly susceptible to nitration. Several independent observations demonstrate that the GFD preparation used fulfilled these requirements: (1) the GFD preparation is homogeneous as judged by MALDI-MS (Figure 3A) and reacts stoichiometrically with uPAR (see Materials and Methods), (2) approximately 50% of GFD is recovered in the complex with uPAR in the absence of TNM modification under the conditions used, *i.e.*, a 2-fold molar excess of GFD, and (3) no difference between complexed, uncomplexed, and the original GFD preparation could be detected by amino acid or MALDI-MS analysis in the absence of TNM modification (Table 1).

Quantification of tyrosine modification by amino acid analysis of GFD after TNM modification of the uPAR−GFD mixture demonstrated approximately 90% modification of Tyr^{24} in uncomplexed GFD with no modification detectable in the GFD dissociated from the uPAR−GFD complex (Table 1). MALDI-MS and amino acid analyses showed that no alternative modifications had been introduced into uPAR-complexed GFD on treatment with TNM (Table 1 and Figure 3B). The uncomplexed GFD consistently showed a mass increase of 44.7 Da corresponding to expected change upon introduction of one nitro group. A variable amount of an additional component having a mass approximately 16 Da lower than that of the nitrated derivative was also observed (Table 1 and Figure 3C). Enzymatic peptide mapping of nitrated GFD combined with MALDI-MS detection suggested that this heterogeneity arose due to decomposition of the nitrated tyrosine residue, possibly during sample desorption in the mass spectrometer. Consistent with this interpretation a similar phenomenon was observed by PD-MS analysis of purified peptides derived from uPAR domain I, where the major peaks corresponding to the nitrated peptides were always uniquely associated with minor peaks also exhibiting a loss of 16 Da (data not shown).

Ligand Protection of uPAR during Chemical Modification. The extent of tyrosine modification of uPAR in the experiment shown in Figure 2 was determined by amino acid analysis (Table 2). Uncomplexed uPAR showed an average tyrosine nitration of 2.4 (Table 2, column 3), in agreement with the TNM titration shown in Figure 1A. In uPAR dissociated from the uPAR−GFD complex this average nitration was reduced to 1.7 (Table 2, column 2), approximating to the protection of a single tyrosine residue under these reaction conditions.

The data shown in Figure 1 suggested that the majority of the uPAR nitration under these conditions was localized in domain I, *i.e.*, Tyr^{57} and Tyr^{87}, indicating that the observed protection is likely to be at one of these positions. Therefore, the various uPAR preparations from Figure 2 were degraded to fragments 1−83, 84−89, and 90−277 by limited proteolysis with trypsin as described earlier and purified by gel filtration (Figure 4, upper panel). Of the two fragments containing single tyrosine residues (1−83 and 84−89), only the former had a reduced absorbancy at 436 nm when uPAR dissociated from GFD was compared to uncomplexed uPAR (Figure 4, fraction B4 compared to C4). This strongly suggests that the observed protection of uPAR nitration by GFD is occurring at Tyr^{57}.

The protection of Tyr^{57} was substantiated by further trypsin digestion of fractions B4 and C4 (consisting of 1−83 and residual amounts of 1−89) which were combined with the corresponding fractions B5 and C5 (consisting of 84−89) before reversed-phase HPLC. This strategy was used to recover both modified and unmodified tyrosine-containing peptides, and thus directly compare the tyrosine modification of all peptides derived from the sequence 1−89, nitrated peptides being resolved from the corresponding unnitrated peptides in this chromatographic system. Comparison of the chromatograms shown in Figure 4 (lower panel) demonstrates the presence of a nitrated peptide corresponding to residues 54−58 (C9) derived from uncomplexed uPAR, which is absent in the peptides derived from the uPAR−GFD complex. Instead, the latter peptide mixture shows an increased abundance of the corresponding unmodified pep-

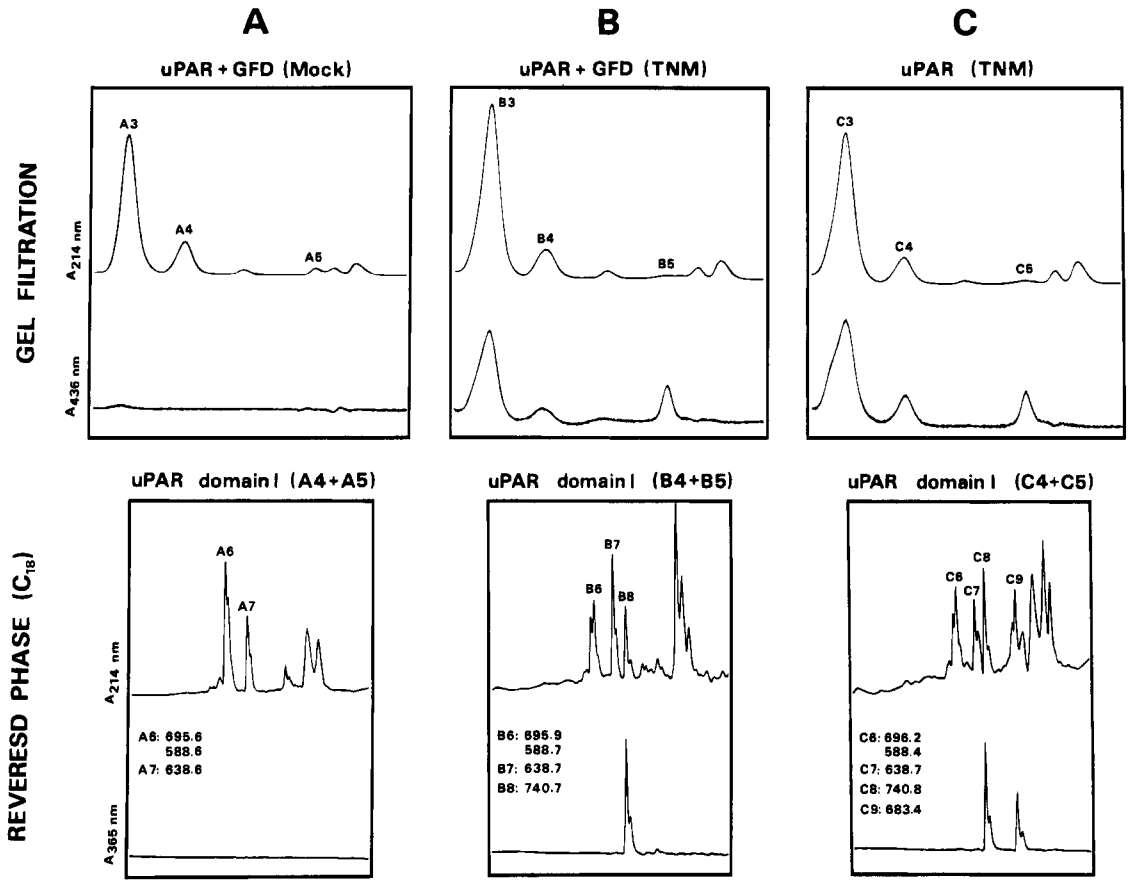

FIGURE 4: Influence of the interaction with GFD on nitration efficiency of Tyr^{57} and Tyr^{87} in uPAR domain I. Fractions containing uPAR from the reversed-phase chromatograms described in Figure 2 were lyophilized, redissolved in 0.2 M NH_4HCO_3 (pH 8), and incubated with trypsin (E:S ~ 1:2000 w/w) for 1 h at 37 °C. The upper panel shows the resulting elution profiles when these tryptic digests were analyzed by Superdex HR75 gel filtration in 0.1 M NH_4HCO_3. Fractions containing residues 1−83 (A4, B4, and C4) were collected, further cleaved by trypsin (E:S ~ 1:25 w/w), and pooled with the corresponding fractions containing residues 84−89 (A5, B5, and C5, respectively). The lower panel shows the elution profiles when these peptide mixtures were analyzed by reversed-phase chromatography (Brownlee C18 column) using acetonitrile as eluent. The identities of the eluted peptides were revealed by determination of their molecular masses by PD-MS analysis as indicated in each chromatogram: fractions A6, B6, and C6 all contained a mixture of the same two peptides, $TTIVR^{30}$ (588.7 Da) and $AVTYSR^{89}$ (695.8 Da). Equal peak intensities were observed by PD-MS for these peptides in A6, whereas the peak intensity of $AVTYSR^{89}$ was reduced to only 20% of the signal for $TTIVR^{30}$ in both B6 and C6. Only one peptide was detected in A7, B7, and C7 corresponding to $TLSYR^{58}$ (638.7 Da). The nitrated peptide $AVTY[NO_2]SR^{89}$ (740.8 Da) was found as the sole constituent of B8 and C8 whereas $TLSY[NO_2]R^{58}$ (683.7 Da) was the only peptide detected in C9.

tide 54−58 (B7 compared to C7). In contrast to the effects on Tyr^{57}, equivalent nitration of peptides containing Tyr^{87} (B8 compared to C8) was evident.

As discussed above, the conditions used for this study were chosen to preferentially modify residues in domain I of uPAR, *i.e.*, Tyr^{57} and Tyr^{87}. However, an average of one out of the four tyrosine residues in domains II + III was also modified (Table 2, column 6). Amino acid analysis of this fragment revealed a reduction in nitration of uPAR domains II + III derived from the uPAR−GFD complex corresponding to an average of 0.3 tyrosine residue (Table 2, column 5). Therefore, from these data it is not possible to completely exclude that GFD may also have some protective influence on a tyrosine residue in domains II + III of uPAR.

DISCUSSION

Protein structure−function relationships have been extensively studied using both chemical modification and site-directed mutagenesis. The interpretation of such studies is, however, often complicated by perturbation of the three-dimensional structure of the native proteins secondary to the introduction of the specific modification or mutation. As we have previously shown that high-affinity binding of uPA to uPAR is potentially sensitive to conformational changes in uPAR (Ploug et al., 1994), such methods may also give ambiguous results when the uPAR−uPA interaction is studied. We have therefore chosen to identify residues participating in the molecular interface between uPAR and uPA by observing the protection of such residues from chemical modification. Our previous studies have indicated that the uPA binding site of uPAR has a hydrophobic nature and that aromatic residues participate in this binding site (Ploug et al., 1994). Therefore, the involvement of tyrosine residues was investigated, the recombinant soluble form of uPAR used containing a total of six tyrosines, two of which are in the NH_2-terminal domain I (residues 1−89). The isolated GFD module of uPA was used in these experiments rather than the intact protein, as they have been shown to have indistinguishable receptor binding characteristics (Mazar et al., 1992) and GFD contains only one tyrosine residue compared to 18 in uPA, much simplifying the identification of individual residues.

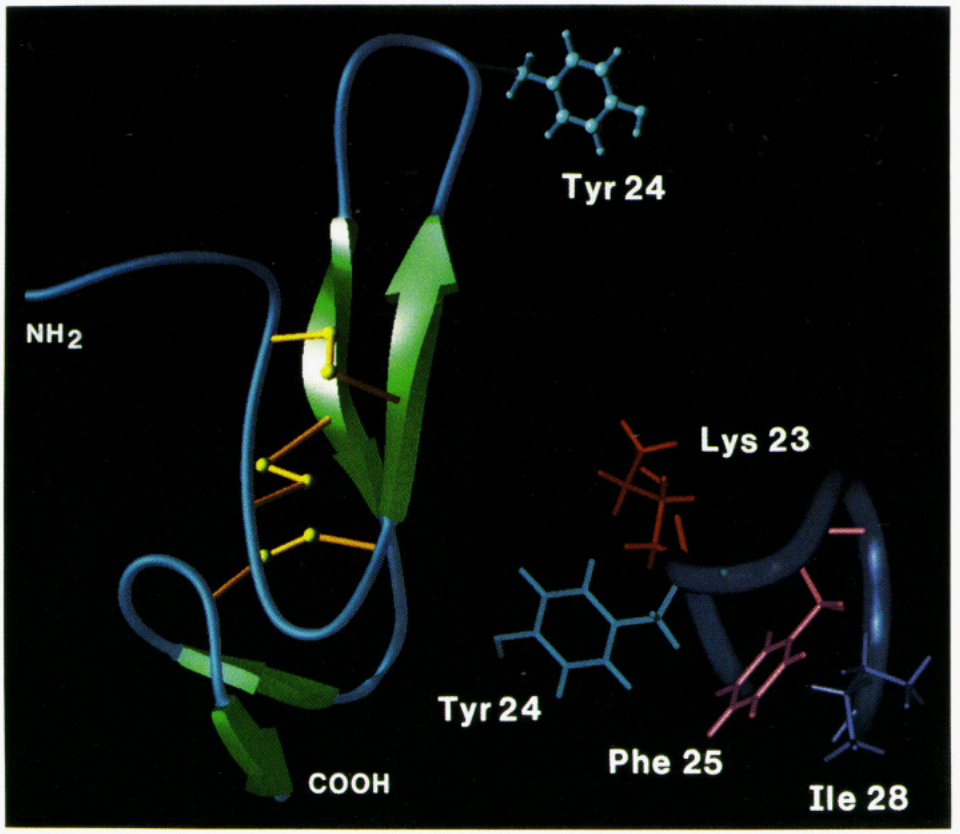

		10										20										30										40									
Human	**uPA:**	N	C	D	C	L	N	G	G	T	C	V	S	N	K	Y	F	S	N	I	H	W	C	N	C	P	K	K	F	G	G	Q	H	C	E	I	D	K
Baboon	**uPA:**	D	C	G	C	L	N	G	G	T	C	M	S	N	K	Y	F	S	S	I	H	W	C	N	C	P	K	K	F	G	G	Q	H	C	E	I	D	K
Porcine	**uPA:**	N	C	G	C	L	N	G	G	K	C	V	S	Y	K	Y	F	S	N	I	Q	R	C	S	C	P	K	K	F	Q	G	E	H	C	E	I	D	T
Bovine	**uPA:**	N	C	G	C	L	N	G	G	K	C	V	T	Y	K	Y	F	S	N	I	Q	R	C	S	C	P	K	K	F	Q	G	E	H	C	E	I	D	T
Murine	**uPA:**	N	C	G	C	Q	N	G	G	V	C	V	S	Y	K	Y	F	S	R	I	R	R	C	S	C	P	R	K	F	Q	G	E	H	C	E	I	D	A
Chicken	**uPA:**	E	C	Q	C	L	N	G	G	T	C	I	T	Y	R	F	F	S	Q	I	K	R	C	L	C	P	E	G	Y	G	G	L	H	C	E	I	D	T
CONSENSUS:		-	C	-	C	-	N	G	G	-	C	-	-	-	-	-	F	S	-	I	-	-	C	-	C	P	-	-	-	-	G	-	H	C	E	I	D	-

FIGURE 5: Three-dimensional structure of human GFD and alignment of GFD sequences from different species. Panel A (top) shows a schematic representation of the topology of human GFD (residues 6−45) based on the NMR-derived solution structure of ATF (Hansen et al., 1994a). The green arrows represent the β-sheet structures of GFD whereas the ω-loop (Asn^{22}−Ile^{28}) is highlighted by the blue α-carbon backbone with the side chain of the protected Tyr^{24}. Selected side chains of this loop are also shown at a higher magnification. Panel B (bottom): Sequences corresponding to the GFD module of uPA from the following species were aligned manually: human (Günzler et al., 1982), baboon (Au et al., 1990), porcine (Nagamine et al., 1984), bovine (Krätzschmar et al., 1994), murine (Belin et al., 1985), and chicken (Leslie et al., 1990). The amino acid numbering refers to the protein sequence of human uPA and the solid star indicates the position of Tyr^{24} protected from nitration in the uPAR−GFD complex. The shaded area of the human GFD module represents the sequence involved in receptor binding as delineated by synthetic peptides (Appella et al., 1987), and the boxed sequence indicates the position of the unique ω-loop found in the GFD module of human uPA (Hansen et al., 1994a).

The data show that all of the tyrosine residues in both molecules are accessible to nitration by TNM, and under the mild conditions chosen for the subsequent experiments an average nitration of 2.4 residues was achieved in uPAR, this nitration being preferentially located in the two tyrosines of the NH_2-terminal domain I. Analysis of the uPAR−GFD complexes under these nitration conditions revealed that tyrosine residues were protected from modification and that the protected residues were located in both uPAR and GFD.

The single tyrosine residue of GFD (Tyr^{24}) was protected from nitration and is centrally situated in the sequence Asp^{12} to Asn^{32} previously identified as being involved in receptor binding using synthetic peptides (Appella et al., 1987). Circumstantial evidence has suggested that this residue is involved in receptor binding as proteolytic cleavages located immediately COOH terminally to either Tyr^{24} or Phe^{25} render the GFD module of ATF inactive (Appella et al., 1987) and ^{125}I-labeling of the isolated GFD module similarly destroys its receptor binding ability (Rabbani et al., 1992). However, neither of these observations can be taken as unequivocal evidence for the involvement of Tyr^{24} in the molecular interaction with uPAR as these direct modifications could have a profound effect on the conformation of the GFD module. This is particularly the case for proteolytic cleavages in GFD, as these lead to a relatively large increase in its hydrodynamic volume as evaluated by gel filtration using Superdex 30 (unpublished observations). In the present study the use of the protection assay overcomes these problems

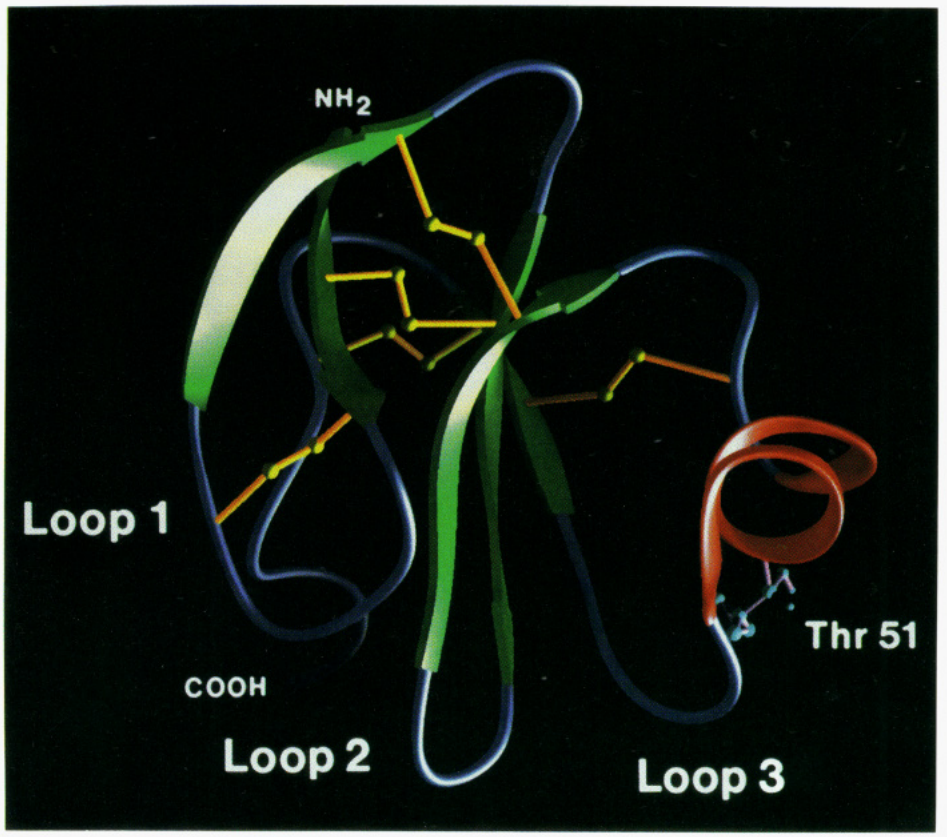


```
                    1                  10                  20                  30                  40
Human     uPAR:  L R C M Q C K T . N G D C R . V E E C A L G Q D L C R T T I V R L W E E G E E L E L V E K S C
Bovine    uPAR:  L R C L Q C E N . T T S C S . V E E C T P G Q D L C R T T V L S V W E G G N E M N V V R K G C
Murine    uPAR:  L Q C M Q C E S . N Q S C L . V E E C A L G Q D L C R T T V L R E W Q D D R E L E V V T R G C
Rat       uPAR:  L R C I Q C E S . N Q D C L . V E E C A L G Q D L C R T T V L R E W E D A E E L E V V T R G C

Human     CD59:  L Q C Y N C P N P T A D C K T A V N C S S D F D A C L I T K A . . . . . G L Q V Y N K . C

CONSENSUS for
Ly-6 superfamily:  - - C - - C . . . . . C . . . . . C - - - - - - C . . . . . . . . . . . . . . . . . . . . C

                    50                  ★ 60                70                  80                  ☆ 90
Human     uPAR:  T H S E K T N R T L S Y R T G L K I T S L T E V V C G L D L C N Q G N S G . R A V T Y S R S R
Bovine    uPAR:  T H P D K T N R S M S Y R A A D Q I I T L S E T V C R S D L C N K P N P G . R D A T V S R N R
Murine    uPAR:  A H S E K T N R T M S Y R M G S M I I S L T E T V C A T N L C N R P R P G A R G R A F P Q G R
Rat       uPAR:  L H K E K T N R T M S Y R M G S V I V S L T E T V C A T N L C N R P R P G A R G R P F P R G R

Human     CD59:  W K F E H C N F N D V T T R L R E N . E L T Y Y C C K K D L C N F N E Q L E N  - glycolipid

CONSENSUS for
Ly-6 superfamily:  . . . . . C . . . . . . . . . . . . . . . . . . . . C C - - - - C N
```

FIGURE 6: Three-dimensional structure of human CD59 and alignment of sequences of the NH_2-terminal uPAR domain I from different species and human CD59. The NMR-derived solution structure of human CD59, a putative structural homolog of the individual domains of uPAR, is shown schematically in panel A (top) (Fletcher et al., 1994). The helical element of CD59, absent from the structures of the homologous snake venom α-neurotoxins, is highlighted by a red ribbon α-carbon backbone. The side chain of Thr^{51} is also shown being located at a position equivalent to that of Tyr^{57} in human uPAR domain I. In panel B (bottom) is shown a sequence alignment of uPAR domain I (including the linker region) from four different species: human (Roldan et al., 1990), bovine (Krätzschmar et al., 1993), murine (Kristensen et al., 1991), and rat (Rabbani et al., 1994). Also included in this sequence alignment is human CD59 (Davies et al., 1989)—a glycolipid anchored, single-domain protein belonging to the Ly-6/uPAR superfamily. The helical secondary structure of CD59 is highlighted by the boxed sequence. The amino acid numbering refers to the protein sequence of human uPAR, and the solid star indicates the positions of the protected Tyr^{87} whereas the open star marks the unprotected Tyr^{87} in the interdomain linker region. Cysteine residues are marked with shaded boxes, and the conserved disulfide pairing (Ploug et al., 1993) is shown in the consensus sequence. Invariant spacings between cysteines (- - -) as well as those tolerant to gap events (•••) are shown.

as the GFD module remains receptor bound during the modification procedure and is only dissociated from the receptor after removal of TNM.

The tyrosine that is protected during interaction with the receptor is strictly conserved among the GFD modules of uPA from mammalian species and is only conservatively substituted to phenylalanine in the chicken (Figure 5B). From these data we propose that Tyr^{24} and the adjacent Phe^{25} in the GFD module represent an exposed aromatic/hydrophobic patch forming the core of the receptor-binding site. Such properties are consistent with the ability of GFD to compete the binding of ANS to a surface-exposed hydrophobic site on uPAR that is intimately related to the uPA binding site (Ploug et al., 1994). The recently solved solution structure of the NH_2-terminal fragment of uPA (comprising both the GFD and kringle modules) (Hansen et al., 1994a) confirms that Tyr^{24} and Phe^{25} form a patch of high surface hydrophobicity in which Ile^{28} also participates, as illustrated in Figure 5A. These residues are located in an exposed ω-loop (Asn^{22} to Ile^{28}) connecting the two strands of the major antiparallel β-sheet of the GFD module (Figure 5A). This loop is the most flexible region within the GFD module (Hansen et al., 1994b) and constitutes the largest structural difference between the GFD module of uPA and those of EGF and TGF-α. Thus the structural features of this part of the GFD module also make it a good candidate for the uPAR binding site. The properties of this region are in good accordance with the recently proposed general principle that patches of high hydrophobicity occur at protein−protein interfaces and contribute the majority of the binding free energy (Young et al., 1994; Clackson & Wells, 1995).

Structural elements within uPAR participating in the interaction with uPA are as yet largely unidentified. It has been demonstrated, however, that the NH_2-terminal domain I of uPAR (residues 1−87) contains the principal binding determinants since (1) the ability to form a specific covalent cross-linked conjugate with ^{125}I-labeled ATF using the homobifunctional chemical cross-linker *N,N'*-disuccinimidyl suberate has been mapped to uPAR domain I (Behrendt et al., 1991), (2) a monoclonal anti-uPAR antibody (clone R3) recognizing domain I abrogates concomitant uPA binding (Rønne et al., 1991), and (3) the same antibody can titrate the uPAR-dependent enhancement of ANS fluorescence—a fluorophore reporting on the availability of a functional high-affinity binding site for uPA (Ploug et al., 1994). Despite the prominent role of domain I in the ligand interaction a contribution from domains II + III is also necessary as it has been demonstrated that proteolytic cleavage after Tyr^{87} causes a more than 2000-fold reduction in the receptor affinity for uPA (Ploug et al., 1994). Data from ANS fluorescence experiments indicate that the binding site for uPA is correlated to the presence of an exposed hydrophobic area on uPAR (Ploug et al., 1994).

In the present study we have shown that Tyr^{57} of uPAR is protected from nitration when intact three-domain uPAR is complexed to the GFD module of uPA, whereas Tyr^{87} positioned in the linker region connecting domains I and II is nitrated irrespective of the interaction with GFD. The latter finding is consistent with the observation that the Tyr^{87}−Ser^{88} peptide linkage retains its susceptibility to chymotrypsin cleavage when uPAR is in complex with uPA (unpublished results). From the sequence alignments of uPAR domain I from different species (Figure 6B) it is evident that Tyr^{57} is a conserved residue whereas Tyr^{87} is located at a nonconserved position. In the absence of experimental data concerning the three-dimensional structure of uPAR it may be informative to draw comparisons with the structures solved for CD59 (another member of the Ly-6/uPAR superfamily) and the homologous snake venom α-neurotoxins. Several independent properties are common to these proteins, making it probable that they adopt a similar overall folding topology—as reviewed (Ploug & Ellis, 1994). The most significant difference between the solution structure of CD59 (Fletcher at al., 1994, Kieffer et al., 1994) and the structures solved for numerous α-neurotoxins [reviewed by Endo and Tamiya (1991)] is the presence of a helical segment in loop 3 of the CD59 molecule (Figure 6A) which is not present in any of the α-neurotoxin structures. Sequence alignment predicts that Tyr^{57}, the residue protected on binding to GFD, is located in the area in uPAR domain I equivalent to this unique helical element and at a position corresponding to Thr^{51} in the CD59 sequence (Figure 6A). However, the exact location of this residue cannot be unequivocally deduced from the sequence alignment due to the presence of a single residue insertion in the uPAR sequences and the unique absence of an otherwise strictly conserved disulfide bond in uPAR domain I. As can be seen from the structure of CD59 (Figure 6) this disulfide bond is situated close to the globular core of the molecule where it "closes" loop 3. It has been previously speculated that the lack of these cysteine residues could be of functional consequence for uPAR (Ploug & Ellis, 1994) which is in accordance with the present mapping of the GFD interaction site to this region of uPAR. Current studies of the ligand-binding properties of a mutant uPAR with the lacking disulfide bond introduced (Thr^{51}→Cys and Val^{70}→Cys) and additional chemical protection analysis of other amino acids intimately involved in ligand binding will enable the further delineation of the uPA binding site of uPAR.

ACKNOWLEDGMENT

We thank Dr. D. Saunders (Grünenthal, Germany) for the generous gift of recombinant pro-uPA, Dr. S. W. Fesik (Abbott Laboratories, Chicago, IL) for providing us with the NMR coordinates of ATF before their release from the Brookhaven Protein Data Bank, Dr. M. Fletcher (Laboratory of Molecular Biology, Cambridge, U.K.) for providing us with the NMR coordinates of CD59, A. Wacey (Thrombosis Research Institute, London, U.K.) for assistance with molecular graphics, Dr. U. Weidle (Boehringer Mannheim, Mannheim, Germany) for the construction of the transfected CHO cells secreting the truncated, soluble uPAR and Dr. A L. Jensen (Department of Protein Chemistry, Copenhagen University, Copenhagen, Denmark) for performing amino acid analyses. Helle Hymøller Hald, Lene Skov, and John Post are thanked for excellent technical assistance.

REFERENCES

Appella, E., Robinson, E. A., Ullrich, S. J., Stoppelli, M. P., Corti, A., Cassani, G., & Blasi, F. (1987) *J. Biol. Chem. 262*, 4437−4440

Au, Y. P. T., Wang, T. W., & Clowes, A. W. (1990) *Nucleic Acids Res. 18*, 3411.

Barkholt, V., & Jensen, A. (1989) *Anal. Biochem. 177*, 318−322.

Beavis, R. C., Chaudhary, T., & Chait, B. T. (1992) *Org. Mass Spectrom. 27*, 156−158.

Behrendt, N., Ploug, M., Patthy, L., Houen, G., Blasi, F., & Danø, K. (1991) *J. Biol. Chem. 266*, 7842−7847.
Belin, D., Vassali, J.-D., Combépine, C., Godeau, F., Nagamine, Y., Reich, E., Kocher, H. P., & Duvoisin, R. M. (1985) *Eur. J. Biochem. 148*, 225−232.
Clackson, T., & Wells, J. A. (1995) *Science 267*, 383−386.
Cuatrecasas, P., Fuchs, S., & Anfinsen, C. B. (1968) *J. Biol. Chem. 243*, 4787−4798.
Danø, K., Behrendt, N., Brünner, N., Ellis, V., Ploug, M., & Pyke, C. (1994) *Fibrinolysis 8* (Suppl. 1), 189−203.
Davies, A., Simmons, D. L., Hale, G., Harrison, R. A., Tighe, H., Lachmann, P. J., & Waldmann, H. (1989) *J. Exp. Med. 170*, 637−654.
Ellis, V., Pyke, C., Eriksen, J., Solberg, H., & Danø, K. (1992) *Ann. N.Y. Acad. Sci. 667*, 13−31.
Endo, T., & Tamiya, N. (1991) in *Snake Toxins* (Harvey, A. L., Ed.) pp 165−222, Pergamon Press, New York.
Fletcher, C. M., Harrison, R. A., Lachmann, P. J., & Neuhaus, D. (1994) *Structure 2*, 185−199.
Günzler, W. A., Steffens, G. J., Otting, F., Kim, S. A., Frankus, E., & Flohe, L. (1982) *Hoppe-Seyler's Z. Physiol. Chem. 363*, 1155−1165.
Hansen, A. P., Petros, A. M., Meadows, R. P., Nettesheim, D. G., Mazar, A. P., Olejniczak, E. T., Xu, R. X., Pederson, T. M., Henkin, J., & Fesik, S. W. (1994a) *Biochemistry 33*, 4847−4864.
Hansen, A. P., Petros, A. M., Meadows, R. P., & Fesik, S. W. (1994b) *Biochemistry 33*, 15418−15424.
Kieffer, B., Driscoll, P. C., Campbell, I. D., Willis, A. C., van der Merve, P. A., & Davis, S. J. (1994) *Biochemistry 33*, 4471−4482
Krätzschmar, J., Haendler, B., Kojima, S., Rifkin, D. B., & Schleuning, W.-D. (1993) *Gene 125*, 177−183.
Kristensen, P., Eriksen, J., Blasi, F., & Danø, K. (1991) *J. Cell Biol. 115*, 1763−1771.
Leslie, N. D., Kessler, C. A., Bell, S. M., & Degen, J. L. (1990) *J. Biol. Chem. 265*, 1339−1344.
Lundblad, R. L., & Noyes, C. N. (1984) in *Chemical Reagents for Protein Modification*, pp 73−103, CRC Press, Boca Raton, FL.
Mazar, A. P., Buko, A., Petros, A. M., Barnathan, E. S., & Henkin, J. (1992) *Fibrinolysis 6* (Suppl. 1), 49−55.
Murphy, G., Atkinson, S., Ward, R., Gavrilovic, J., & Reynolds, J. J. (1992) *Ann. N.Y. Acad. Sci. 667*, 1−12.
Nagamine, Y., Pearson, D., Altus, M. S., & Reich, E. (1984) *Nucleic Acids Res. 12*, 9525−9541.
Nielsen, L. S., Kellerman, G. M., Behrendt, N., Picone, R., Danø, K., & Blasi, F. (1988) *J. Biol. Chem. 263*, 2358−2363.
Palfree, R. G. E. (1991) *Immunol. Today 12*, 170−171.
Ploug, M., & Ellis, V. (1994) *FEBS Lett. 349*, 163−168.
Ploug, M., Rønne, E., Behrendt, N., Jensen, A., Blasi, F., & Danø, K. (1991a) *J. Biol. Chem. 266*, 1926−1936.
Ploug, M., Behrendt, N., Løber, D., & Danø, K. (1991b) *Semin. Thromb. Hemostasis 17*, 183−193.
Ploug, M., Stoffer, B., & Jensen, A. L. (1992) *Electrophoresis 13*, 148−153.
Ploug, M., Kjalke, M., Rønne, E., Weidle, U., Høyer-Hansen, G., & Danø, K. (1993) *J. Biol. Chem. 268*, 17539−17546.
Ploug, M., Ellis, V., & Danø, K. (1994) *Biochemistry 33*, 8991−8997.
Rabbani, S. A., Mazar, A., Bernier, S. M., Haq, M., Bolivar, I., Henkin, J., & Goltzman (1992) *J. Biol. Chem. 267*, 14151−14156.
Rabbani, S. A., Rajwans, N., Acharou, A., Murthy, K. K., & Goltzman, D. (1994) *FEBS Lett 338*, 69−74.
Roepstorff, P. (1994) in *Cell Biology: A Laboratory Handbook* (Celis, J., Ed.) Academic Press, Orlando, FL (in press).
Roldan, A. L., Cubellis, M. V., Mascucci, M. T., Behrendt, N., Lund, L. R., Danø, K., Appella, E., & Blasi, F. (1990) *EMBO J. 9*, 467−474.
Rønne, E., Behrendt, N., Ellis, V., Ploug, M., Danø, K., & Høyer-Hansen, G. (1991) *FEBS Lett. 288*, 233−236.
Rønne, E., Behrendt, N., Ploug, M., Nielsen, H. J., Wöllisch, E., Weidle, U., Danø, K., & Høyer-Hansen, G. (1994) *J. Immunol. Methods 167*, 91−101.
Sokolovsky, A., Riordan, J. F., & Vallee, B. L. (1966) *Biochemistry 5*, 3582−3589.
Sundqvist, B., Kamensky, I., Håkansson, P., Kjellberg, J., Salehpour, M., Widdiyasekera, S., Fohlmann, J., Peterson, P. A., & Roepstorff, P. (1984) *Biomed. Mass Spectrom. 11*, 242−257.
Young, L., Jernigan, R. L., & Covell, D. G. (1994) *Protein Sci. 3*, 717−729.

BI950857M